

EXPERIMENTAL

Material and Methods

All reactions were carried under inert (nitrogen) atmosphere. Toluene and tetrahydrofuran were distilled from standard drying procedures using benzophenone and sodium while the DMSO was dried over calcium hydride and kept over molecular sieves (4 Å). Glutaric anhydride, boron trifluoride diethyl etherate, triethylamine, *N,N'*-disuccinimidyl carbonate, diethylaminomethyl-polystyrene, and fluorescein free acid were purchased from Sigma Aldrich and used without further purification. 2,4-dimethylpyrrole was obtained from DLD Scientific (South Africa) and it was used as received. The c(RGDyK) was purchased from FutureChem Co, Ltd (Seoul, Korea) and it was used as received. All solvents such as ethanol, DMF, DMSO, DCM and TFA were of HPLC-grade and were all purchased from Sigma Aldrich. The synthesis of dipyrromethene intermediate (Compound **3**) was performed using CEM Discovery SP-microwave reactor, USA. The reactions were monitored using a Thin Layer Chromatography (TLC) Merck 60 F₂₅₄ silica gel aluminium coated sheets and using LC-MS analysis was carried out (Shimadzu 2020 UFLC-MS, Japan), with the following conditions: column: YMC-Triat C18 (150 x 4.6 mm, 5 µm), equipped with a photodiode array detector, SPD-MZOA model and the mobile phase: 0.1 % formic acid in water and acetonitrile operating in gradient mode (5-95% in 9 minutes with a hold for 9 minutes or 5-95% in 15 minutes with a hold for 5 minutes). The compounds that were purified with gravity column chromatography made use silica with mesh particle size, 40-63 µm. For compounds that were purified using SFC were carried out on Sepiatec Prep SFC basic (Germany). All reactions were performed in duplicate. The ¹H, ¹³C, ¹⁹F NMR spectra were recorded on Bruker AVANCE III 400 MHz at room temperature and the chemical shifts were reported relative to deuterated chloroform (δ = 7.26 ppm). High-Resolution Mass Spectra (HRMS) were obtained from Bruker micro-TOF-Q II instrument at ambient temperatures, sample concentration of 1 µg/ml. Optical Imaging was performed using the IVIS Lumina III equipment (Perkin Elmer, USA) at the Preclinical Imaging Facility (Pelindaba, South Africa).

Spectroscopic measurements

Absorption spectra were recorded on the UV-3600 Shimadzu UV-VIS-NIR spectrophotometer with the slit width of 2 nm and the pathlength of the cuvette was 1.0 cm. The fluorescent emission spectra were recorded on the PerkinElmer LS 55 fluorescence spectrophotometer. The fluorescence quantum yield of the synthesized BODIPY derivatives were determined by comparing the absorption and emission spectra of BODIPY derivatives prepared as ethanol solutions (refractive index 1.361) with the standard fluorescein prepared in 0.1 M NaOH solution (refractive index 1.330). As per literature the fluorescent quantum yield for standard fluorescein is reported to be of 0.85.² The stock solutions concentration of 5.0×10^{-4} M were prepared and diluted to 5.0×10^{-6} M which was then diluted to suitable concentrations for the collection of the absorbance and the emission spectra. Measurements obtained for calculating the molar absorptivity and fluorescent quantum yield were taken from the prepared solutions with the concentration between 0.25×10^{-6} M to 1.50×10^{-6} M. These solutions provided the absorbance values that were below 0.11 at each λ_{max} . The absorbance that is below 0.11 is essential to avoid auto-absorbance and false results. The molar absorptivity and fluorescent quantum yield were calculated according to the following equations; (equation 1 and equation 2).

$$A = \epsilon \times b \times c \quad (\text{Equation 1.1})$$

$$\Phi_x = \Phi_{st} \left(\frac{Grad_x}{Grad_{st}} \right) \left(\frac{n_x^2}{n_{st}^2} \right) \quad (\text{Equation 2})$$

Examples

1. Determining the molar absorptivity coefficient (ϵ)

Plot the concentration against the absorbance at λ_{max} of the prepared solutions to find the slope

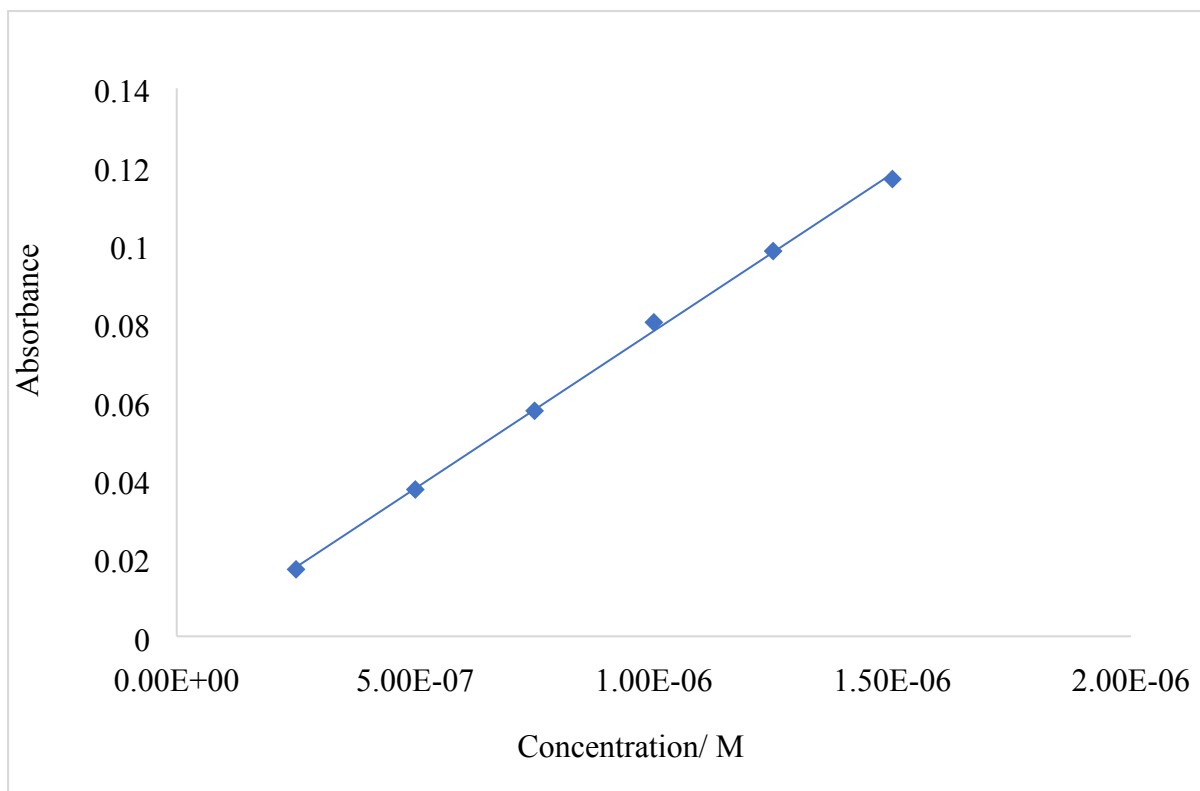


Figure 1 : Plot of Meso-carboxyl BODIPY (**Compound 4**) concentration against the absorbance, solutions prepared in ethanol.

Pathlength $b = 1 \text{ cm}$

Then rearrange **equation 1** to $\epsilon = \frac{A}{C} \times b$, which is equal to the slope of the curve

Therefore; $\epsilon = 80434 \text{ M}^{-1} \cdot \text{cm}^{-1}$

2. Determining the fluorescent quantum yield

Plot the emission versus the absorbance for the samples and the standard to find the slopes

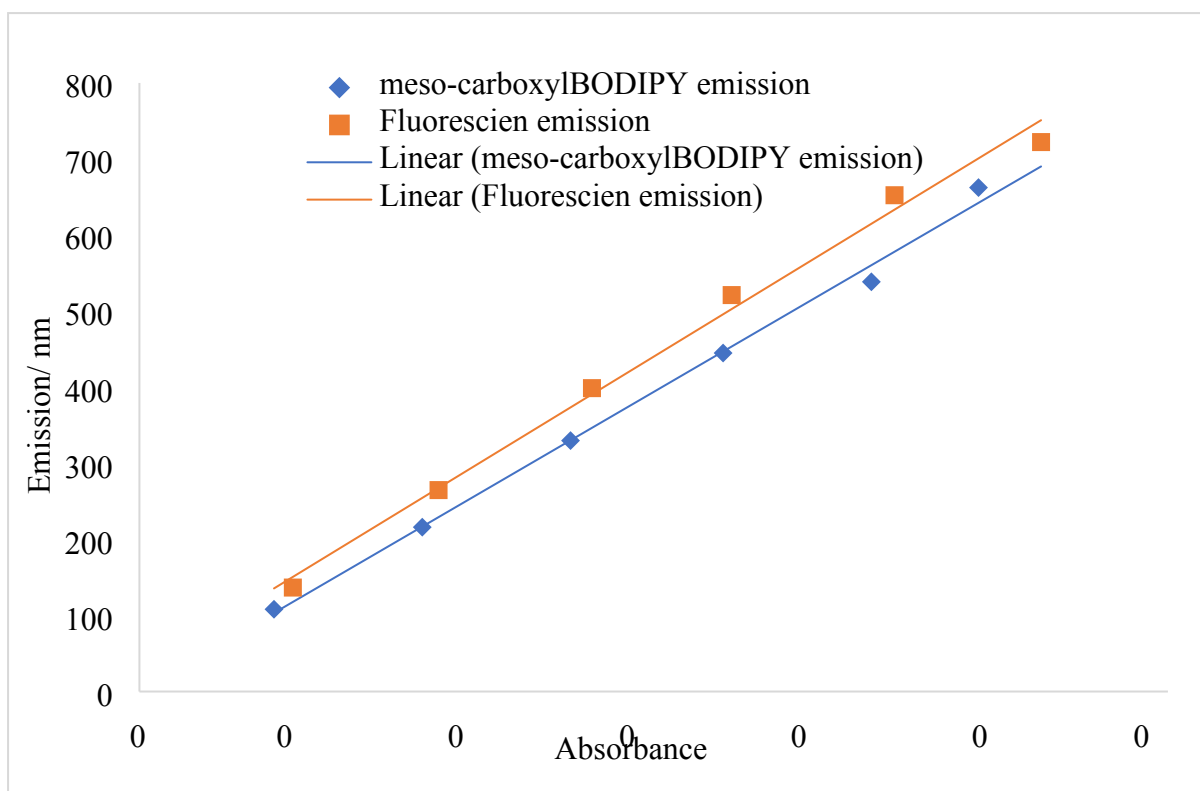


Figure 2: Plot of absorption vs emission for the meso-carboxyl BODIPY (sample/ x) and fluorescein (standard/ st)

Standard fluorescein quantum yield = 0.85

Plug in values to equation 2.

$$\phi_f = 0.8500 \left(\frac{6558}{6877.3} \right) \left(\frac{1.361^2}{1.330^2} \right)$$

$$\phi_f = 0.8487$$

The same procedure was applied for all the other compounds and the results are presented in **Table 1**.

Table 1: Photophysical properties of meso-carboxyl BODIPY dye (**4**), meso-BODIPY-NHS (**8**) and BODIPY peptides (**9-11**) in ethanol.

Compound	$\lambda_{\text{max}}(\text{abs})/\text{nm}$	$\lambda_{\text{max}}(\text{em})/\text{nm}$	$\Delta\lambda/\text{nm}$	$\epsilon / \text{M}^{-1}.\text{cm}^{-1}$	ϕ_f
4	495	504.5	9.5	80434	0.849
8	498	506.0	8.0	75943	0.581

9	496	504.5	8.5	33383	0.609
10	497	505.5	8.5	37189	0.525
11	495	505	10	3716.3	0.508

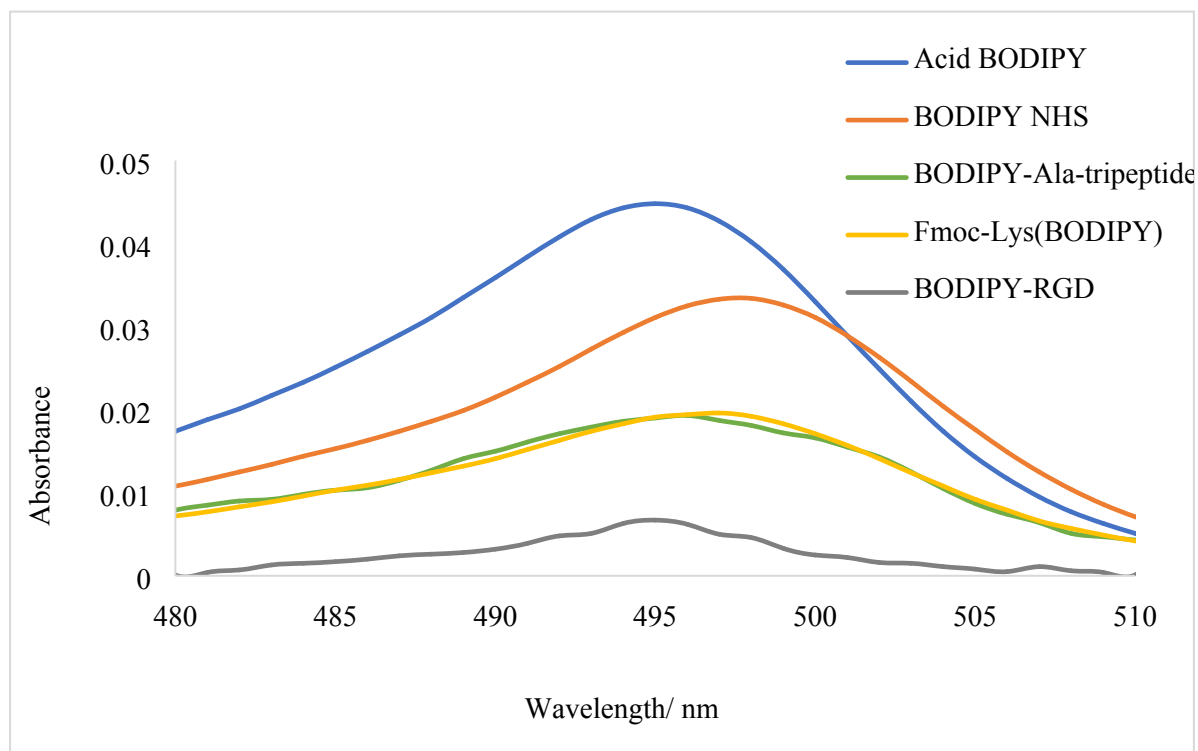


Figure 3: Absorption spectrum of *meso*-carboxyl BODIPY dye, *meso*-BODIPY-NHS and BODIPY peptides (0.5 μ M) in ethanol.

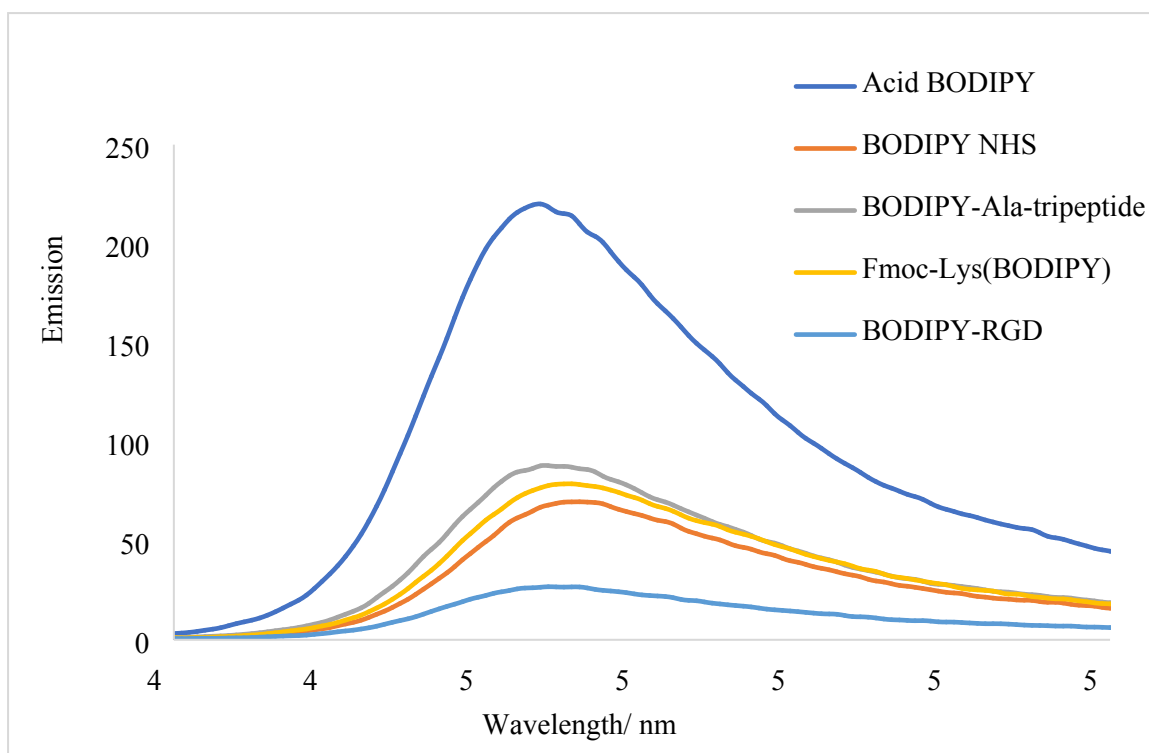


Figure 4: Emission spectrum of *meso*-carboxyl BODIPY dye, *meso*-BODIPY-NHS and BODIPY peptides (0.5 μ M) in ethanol.

BODIPY-c(RGDyK) serum stability

Untreated plasma was obtained from Sprague-Dawley rats and stored at $-80\text{ }^{\circ}\text{C}$. On sample preparation, 990 μL of serum was spiked with 10 μL of 1 mg/mL BODIPY-c(RGDyK), homogenised and incubated at room temperature over a maximum of 4h. A previously published method was employed to obtain and prepare samples at 0 h and thereafter hourly for analysis.¹ Briefly, 100 μL of spiked serum was diluted with 900 μL methanol (MeOH), subjected to vigorous mixing for 1 min and centrifuged at 12000 rpm for 15 min at $4\text{ }^{\circ}\text{C}$. The supernatant was filtered through the hydrophilic-lipophilic balance (HLB, Sigma Aldrich) cartridge as follows: the cartridge matrix was conditioned first with ACN ($2 \times 1\text{ mL}$) followed by MeOH ($2 \times 1\text{ mL}$). The supernatant ($\sim 1\text{ mL}$) was then loaded onto the cartridge and the flow-through was collected into an HPLC vial until the cartridge was dry. The eluent was mixed well and injected on a Thermo Scientific™ | UltiMate™ 3000 UPLC system coupled to Bruker Amazon Speed-Ion Trap Mass Spectrometer with the following separation and detection parameters. The LC separation was achieved using biphenyl 2.7 μm column ($50 \times 4.6\text{ mm}$). The mobile phase were ultra-pure water (0.1 % v/v FA) and acetonitrile (0.1 % v/v FA) at 0.35 mL/min for 10.1 min with the column compartment set to room temperature in the gradient mode of separation. The MS acquisition parameters were positive ion trap

polarity with the endplate offset and the capillary voltage of 600 V and 5000 V. The nebuliser pressure was 1.5 bar and the dry gas was flowing at a flow rate of 8 L/min. Dry heater temperature was 200 °C and the scan range was from m/z 600 to 1100.

Characteristics of the fluorescence signal for BODIPY-c(RGDyK)

In preparation for image acquisition a BODIPY-RGD concentration of 21 nmol/mL for injection) was tested for fluorescence intensity. A manufacture-proposed present for optical imaging using an excitation (ex) at 480 nm paired with emission (em) at 570 nm yielded counts for subsequent BODIPY-RGD injection that were sufficient and well within the allowable count range (minimum of 600 and maximum of 60000) supported by the apparatus calibration. This related to a maximum radiant efficiency of 7.7×10^9 (p/sec/cm²/sr)/μW/cm² (**Figure 5**). Testing of the formulated injection solution included fluorescence image acquisition of a 1 mL plastic syringe carrying 0.3 mL stock solution of BODIPY-RGD (6 nmol); images were acquired with the same camera settings to warrant comparison. Image acquisition was comparing the available filter pairs to determine the peak fluorescence (**Figure 6**).

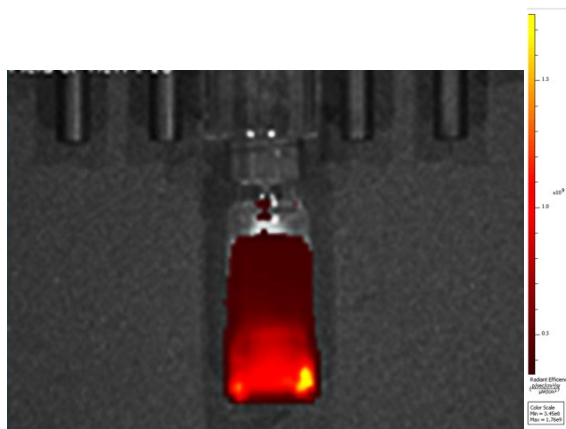


Figure 5: Imaging of BODIPY-c(RGDyK): diluted (21.0 μM). Image acquisition: Lumina IVIS III; exposure time-0.5 s, binning factor -8, F/stop- 2, field of view-10 cm, Ex 480 nm and Em 570 nm

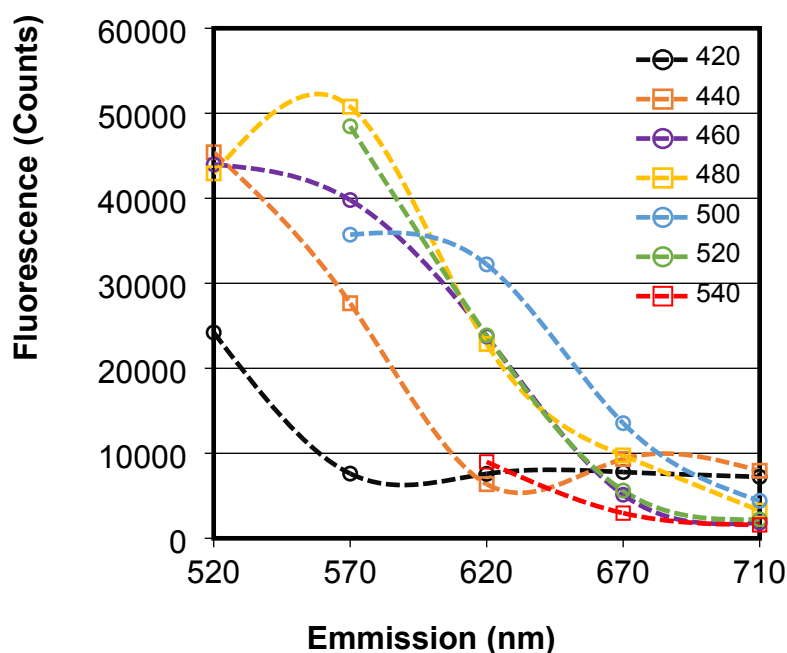


Figure 6: Characterization of BODIPY-c(RGDyK) fluorescence for *in vivo* optical imaging. Image acquisition of BODIPY-c(RGDyK) was performed using IVIS Lumina III of a 1 mL plastic syringe carrying 0.3 mL (6 nmol) BODIPY-c(RGDyK) (exposure time: 0.5 sec, binning factor: 8, f/stop: 2.0, field of view: 10 cm); Legend shows the different excitation wavelengths (available filters of the apparatus).

BODIPY-c(RGDyK)-based Fluorescence Imaging *in vivo*

Eight weeks-old female BALB/c nude (nu/nu) mice were provided the Preclinical Drug Development Platform Vivarium (North West University, Potchefstroom), acclimatized and handled according to the national standards of animal care. All animal experiments were performed in compliance with the North West University's (South Africa) policy on animal use and ethics. The North West University AnimCare Ethics committee granted the ethical clearance with ethics number NWU-00184-18-A5. Three wild type mice were used as control and another two mice were inoculated with MCF-7 – a metastatic breast cancer cell line. At 3-4 weeks after inoculation tumor reached a diameter of approximately 7.5 mm. Tumor dimensions were measured using a calliper, the tumor volume was calculated using the equation: volume (V) = length \times width²/2. No particular animal preparation was required leading up to the administration of BODIPY-c(RGDyK) (1.5-3 nmol/150 μ L) which was injected via the tail vein. The mice were anesthetized using 2% isoflurane carried in an oxygen/air mixture and whole body images were acquired at 3 h and 24 h post injection

BODIPY-c(RGDyK)-based Fluorescence Imaging *ex vivo*

To eradicate interference from the background, *ex vivo* imaging measures were performed also using the optical imaging instrument. Following the final image acquisition mice were euthanized by cervical dislocation. Following blood drainage animal dissection was performed; tumors and multiple organs (heart, liver, spleen, bone, muscle, brain, lung and kidneys) were harvested for excised organ image acquisition using the same *in vivo* imaging equipment and procedures.

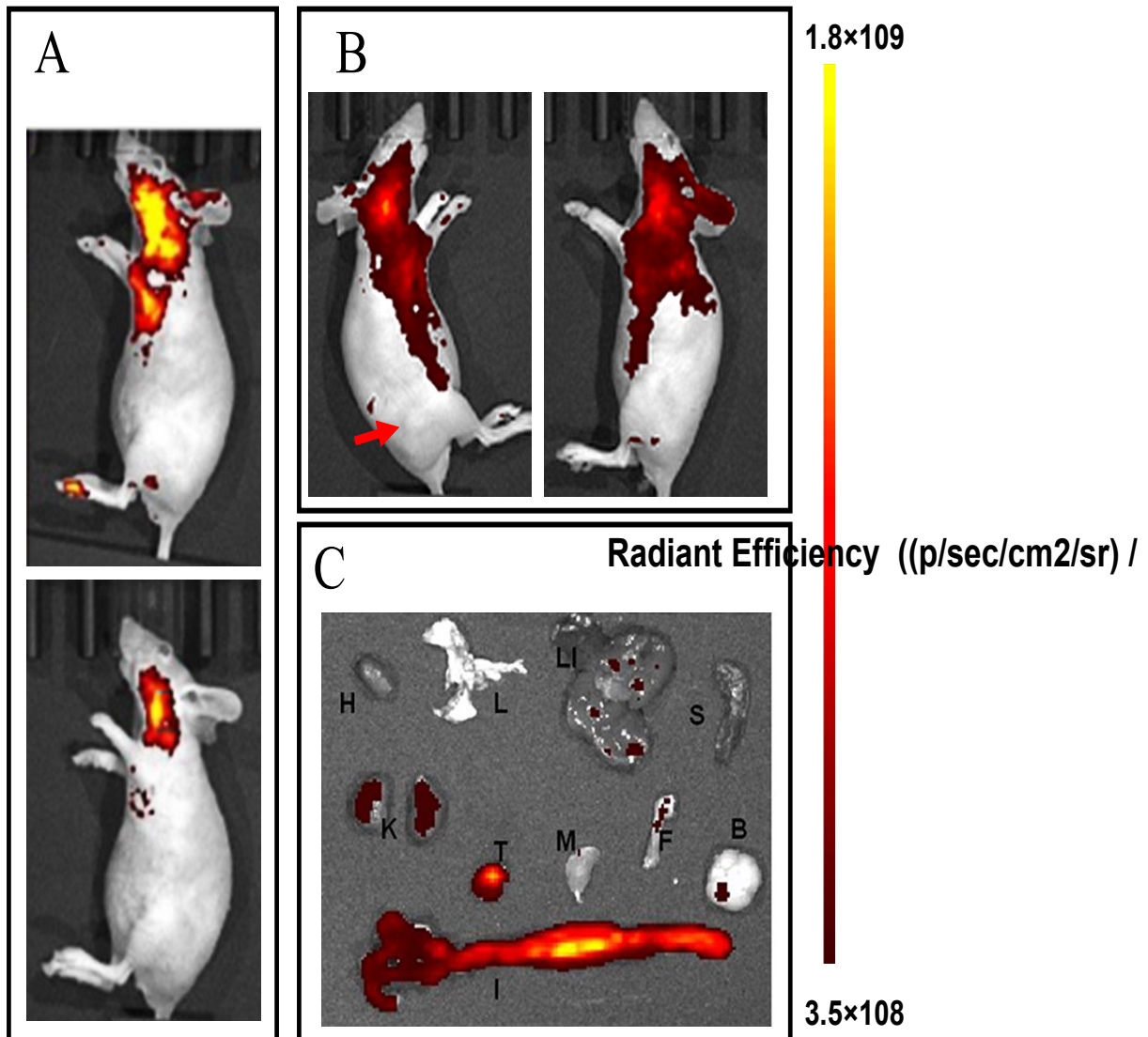


Figure 7: Overview of BODIPY-c(RGDyK) Fluorescence Imaging

Animals received a 0.15 mL bolus of BODIPY-c(RGDyK) via tail vein injection. Images were acquired (field of view = 10.0 - 12.5 cm; Level = high, Ex/Em filter pair (nm) = 480/570) using IVIS Lumina III (Perkin Elmer, Rodgau, Germany) and fluorescence signals were displayed over bright light photos of animals, organs or tissue using Living Image Software 4.5.5 (Perkin Elmer, Rodgau, Germany). Images are corrected for background (counts < 600) and injected dose. (A) Representative images of a wild type balb/c mouse showing BODIPY-c(RGDyK) fluorescence signal (radiant efficiency) *in vivo* at 3 h (top) and 24 h (bottom) following intravenous probe injection; image exposure time (sec) /binning/ f-stop = 0.5/ 8/

2.0. **(B)** *In vivo* tumour visualization of a representative balb/c mouse bearing a MCF-7 tumor xenograft (red arrow indicates tumor location) in the hind flank (left image) compared to the contralateral side (without tumor; right image); image exposure time (sec) /binning/ f-stop = 0.5/ 8/ 2.0. **(C)** Qualitative *ex vivo* organ and tissue analysis; representative biodistribution at 24 h after administration (image exposure time (sec)/ binning/ f-stop = 2.0/ 8/ 2.0). Displayed organ/tissues are: H= heart, L=lung, LI=liver, S=spleen, K=kidneys, T- =tumour, M=muscle, F= femur (bone), B=brain and I= intestines.

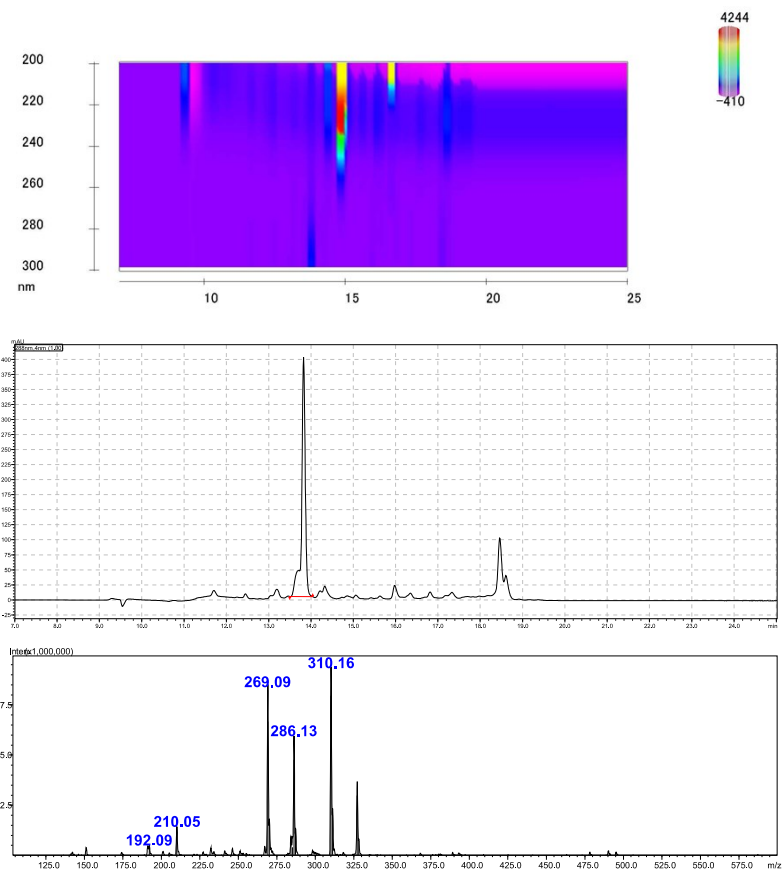


Figure 8: Crude reaction mixture LC-MS-PDA chromatogram of glutaric **3** (~13.8 min) with desired m/z 286 (+ve mode), major UV peak is pyrrole.

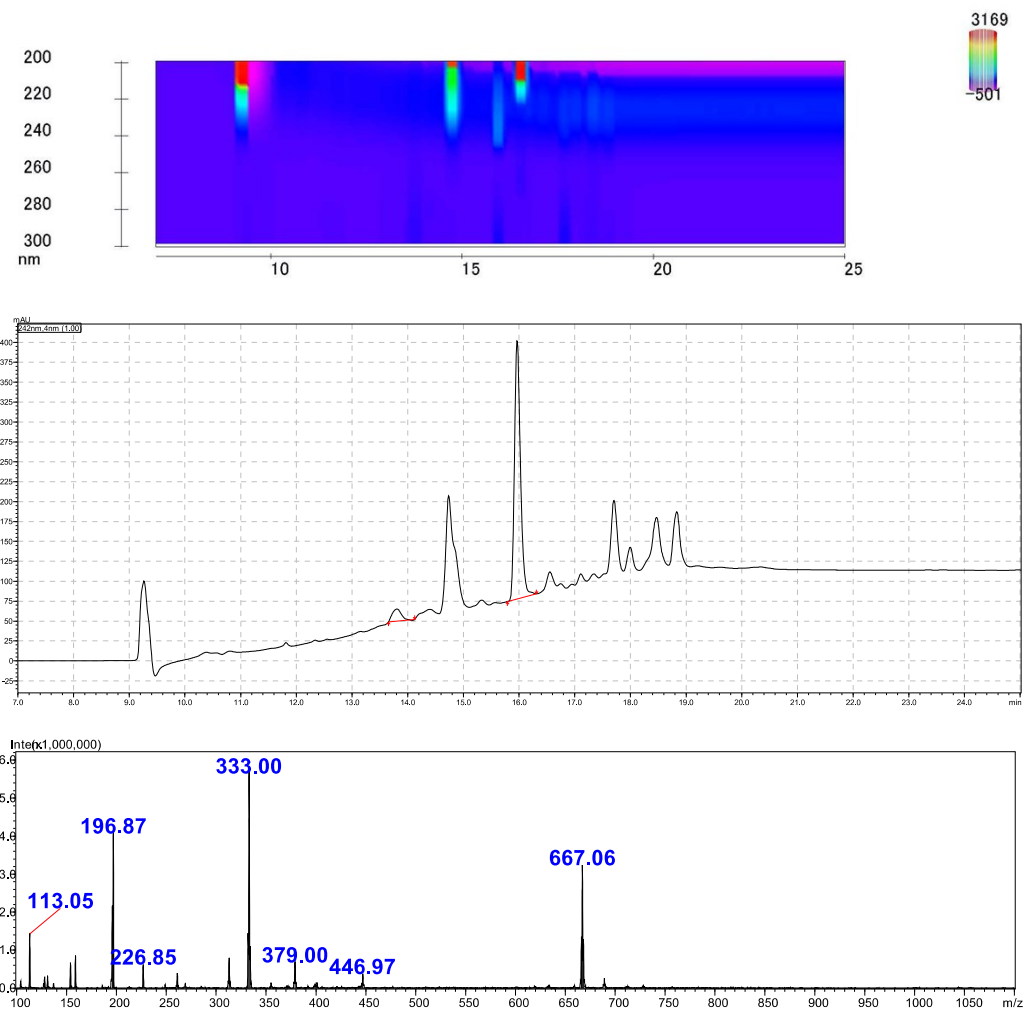


Figure 9: Crude reaction mixture LC-MS-PDA chromatogram of glutaric 4 (~15.9 min) with desired m/z 333 (-ve mode)

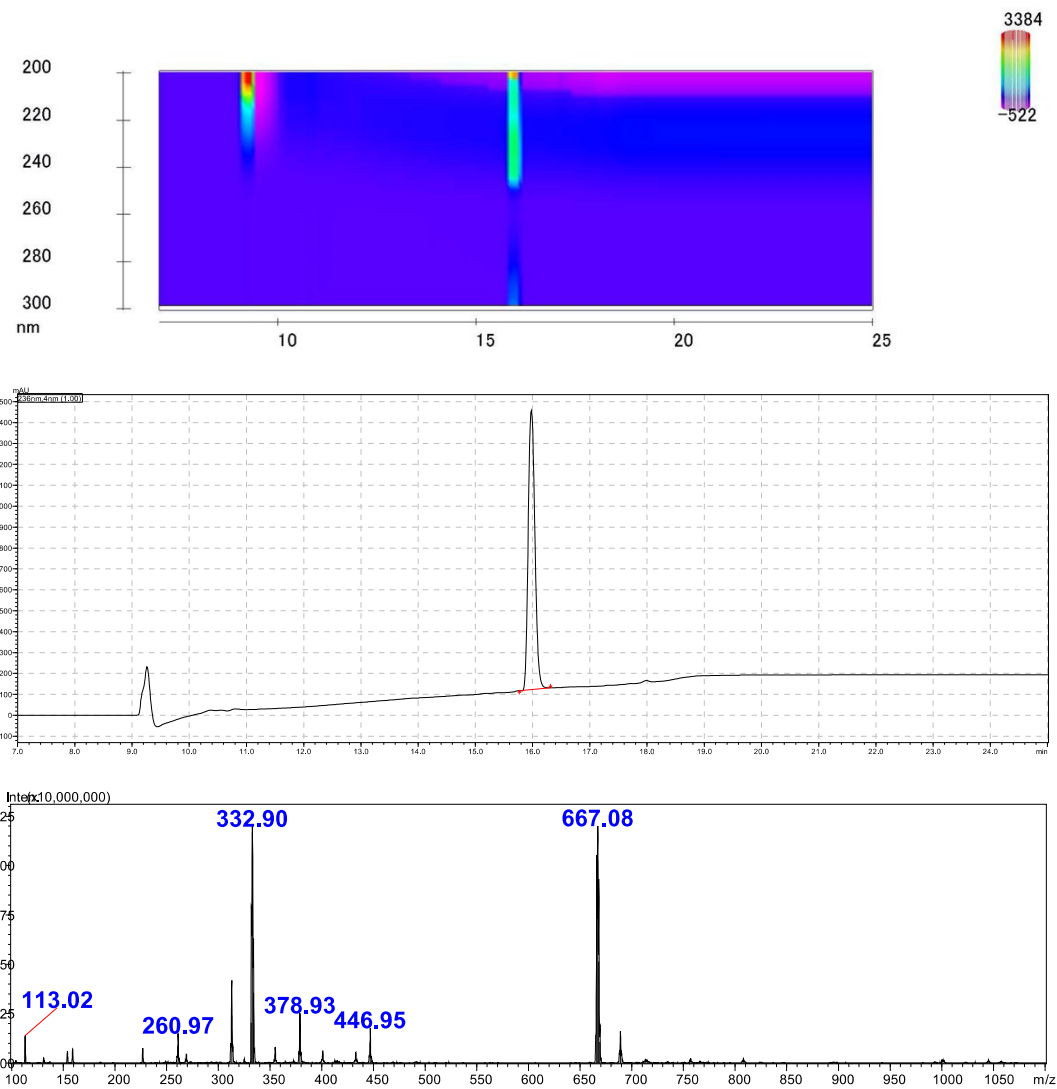


Figure 10: Pure LC-MS-PDA chromatogram of glutaric 4 (~15.9 min) with desired m/z 332.9-333 (-ve mode)

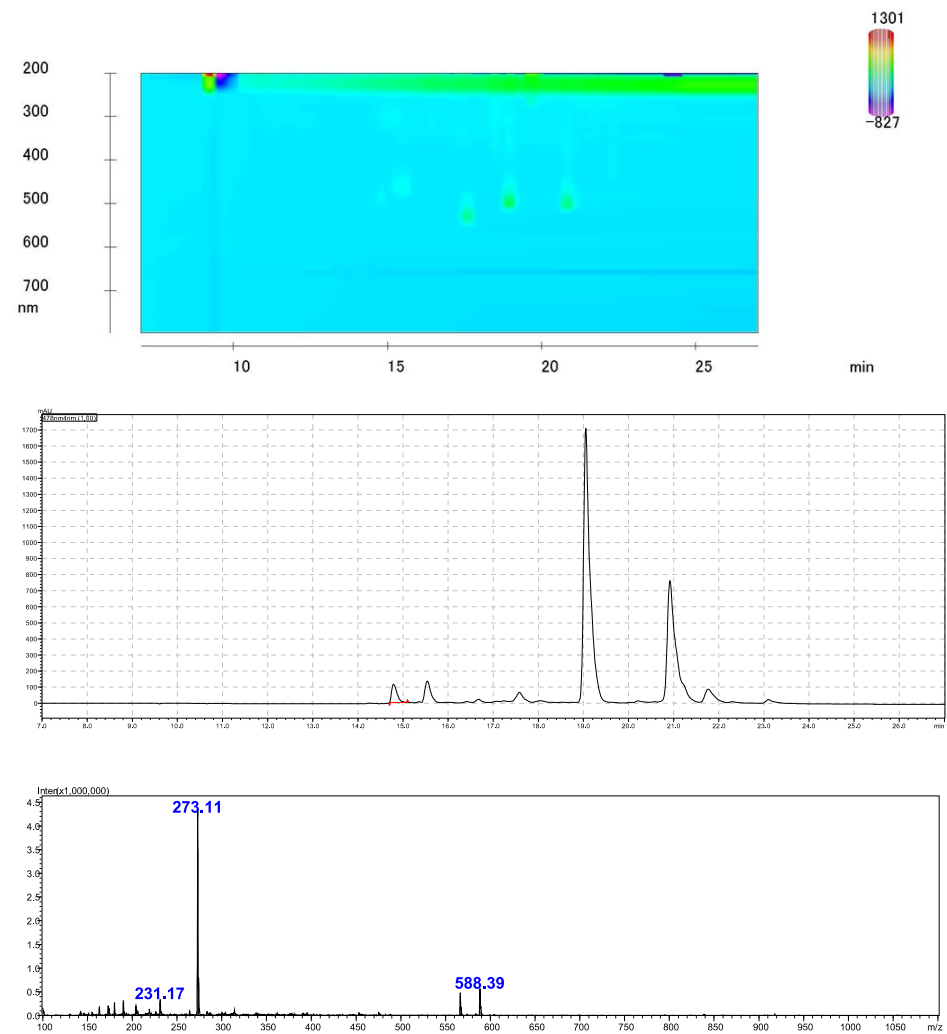


Figure 11: Crude reaction mixture LC-MS-PDA chromatogram of succinic **3** (~14.6 min) with desired m/z 273 (+ve mode)

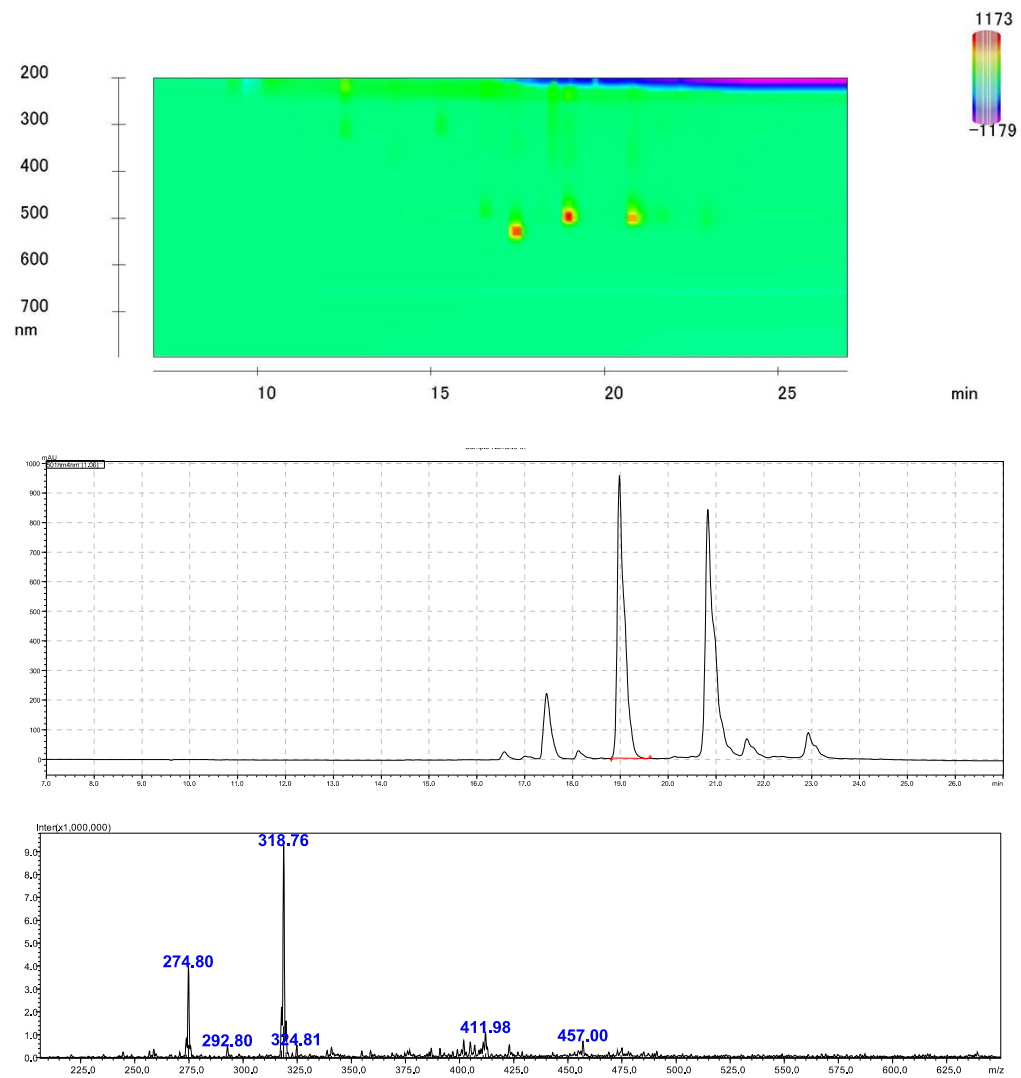


Figure 12: Crude reaction mixture LC-MS-PDA chromatogram of succinic 4 (~19.0 min) with desired m/z 318-319 (-ve mode)

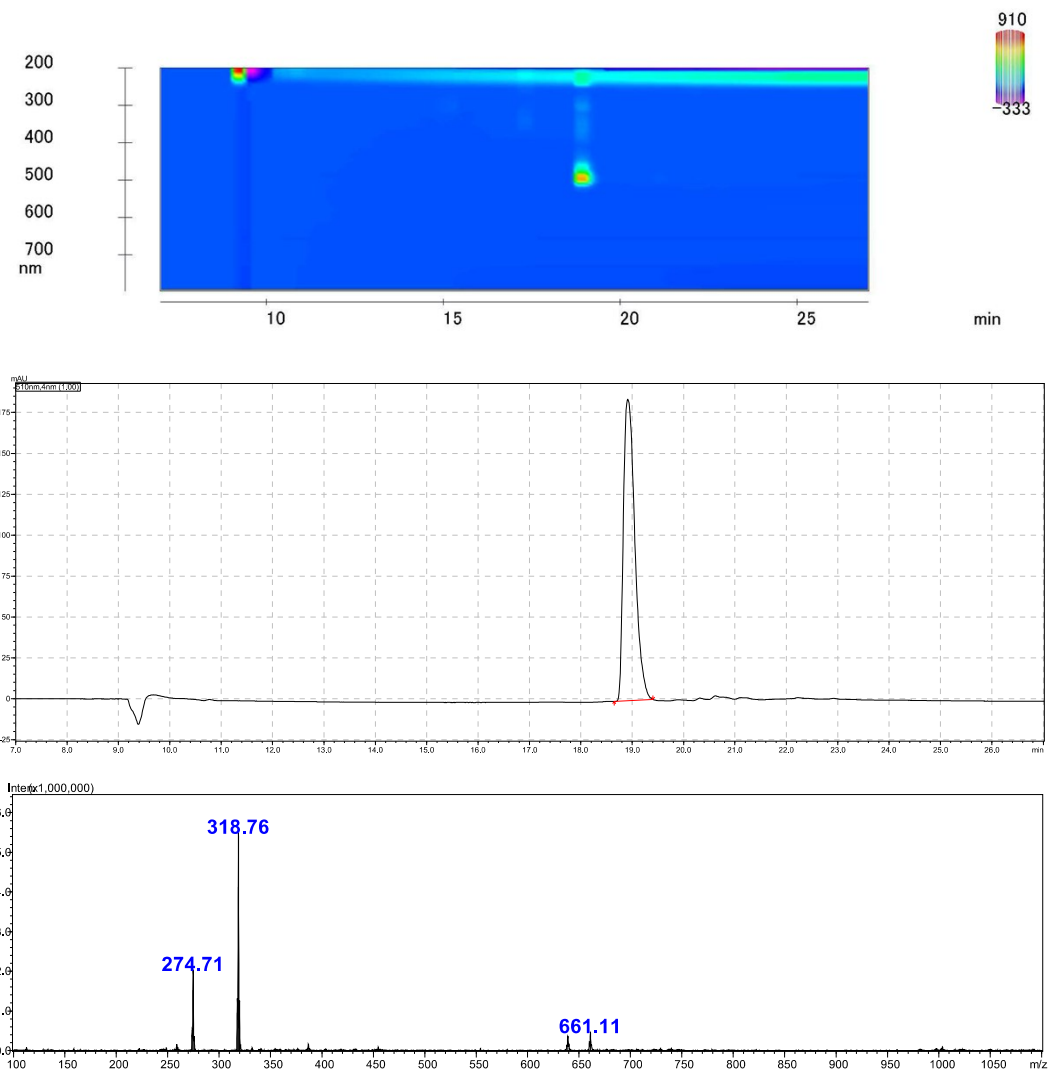


Figure 13: Pure LC-MS-PDA chromatogram of succinic **4** (~19.0 min) with desired m/z 318-319 (-ve mode) or 321 (+ve)

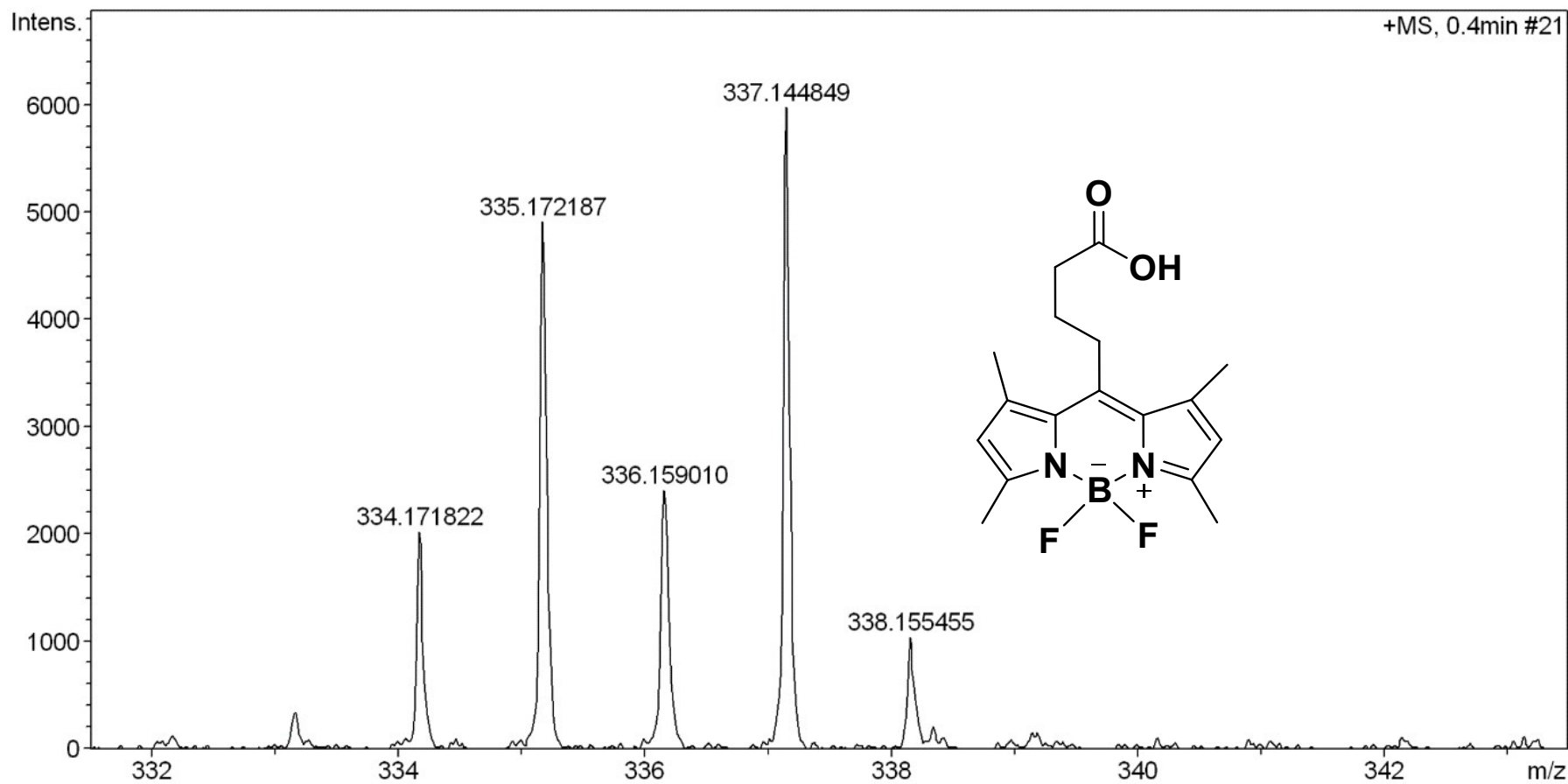


Figure 14: HRMS spectrum for 4-(4,4-Difluoro-1,3,5,7-tetramethyl-4-bora-3a,4a-diaza-s-indacene-8-yl)-butyric Acid (**4**)

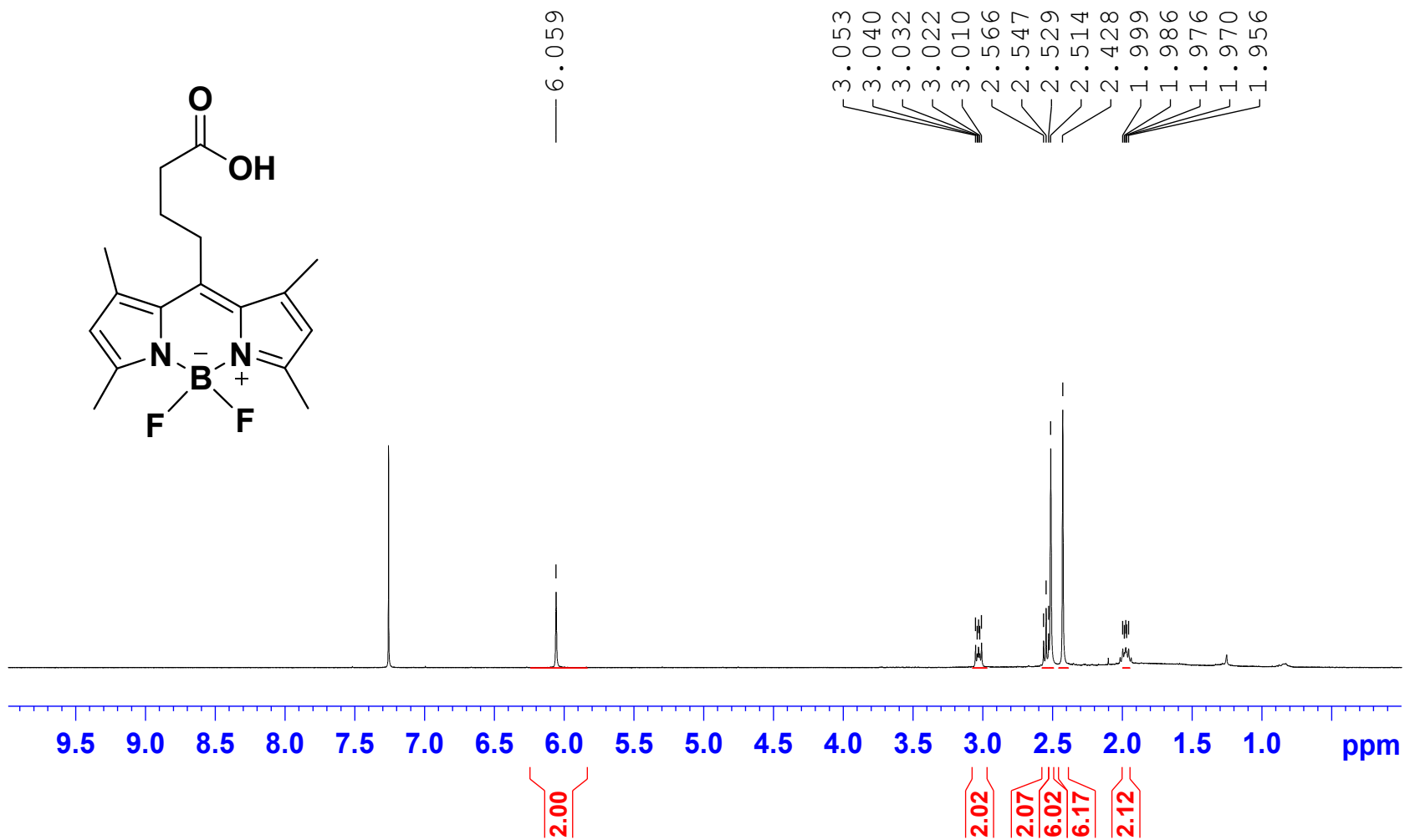


Figure 15: Proton (¹H) NMR spectrum of 4-(4,4-Difluoro-1,3,5,7-tetramethyl-4-bora-3a,4a-diaza-s-indacene-8-yl)-butyric Acid (4)

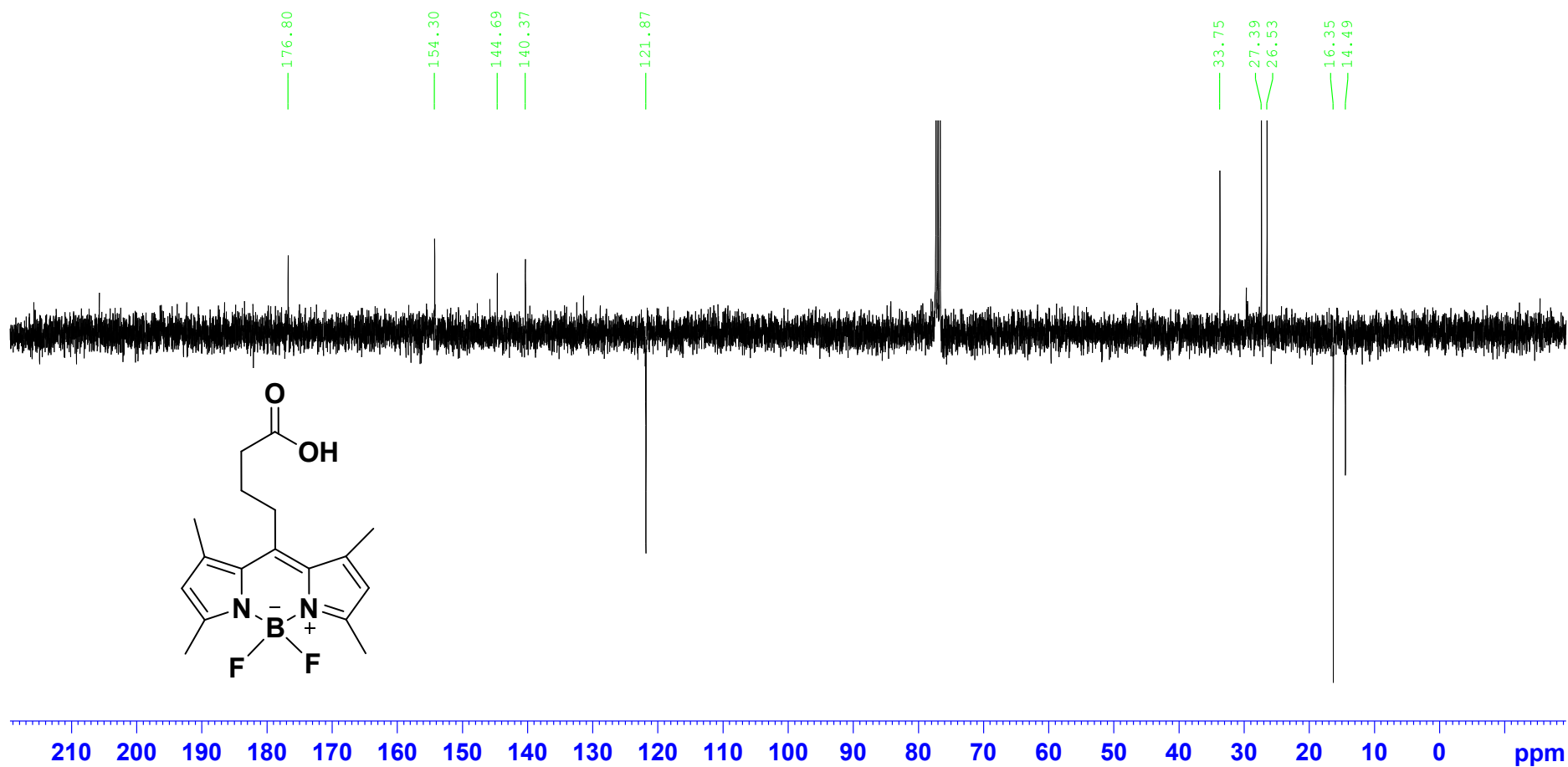


Figure 16: Carbon ^{13}C NMR spectrum 4-(4,4-Difluoro-1,3,5,7-tetramethyl-4-bora-3a,4a-diaza-s-indacene-8-yl)-butyric Acid (4)

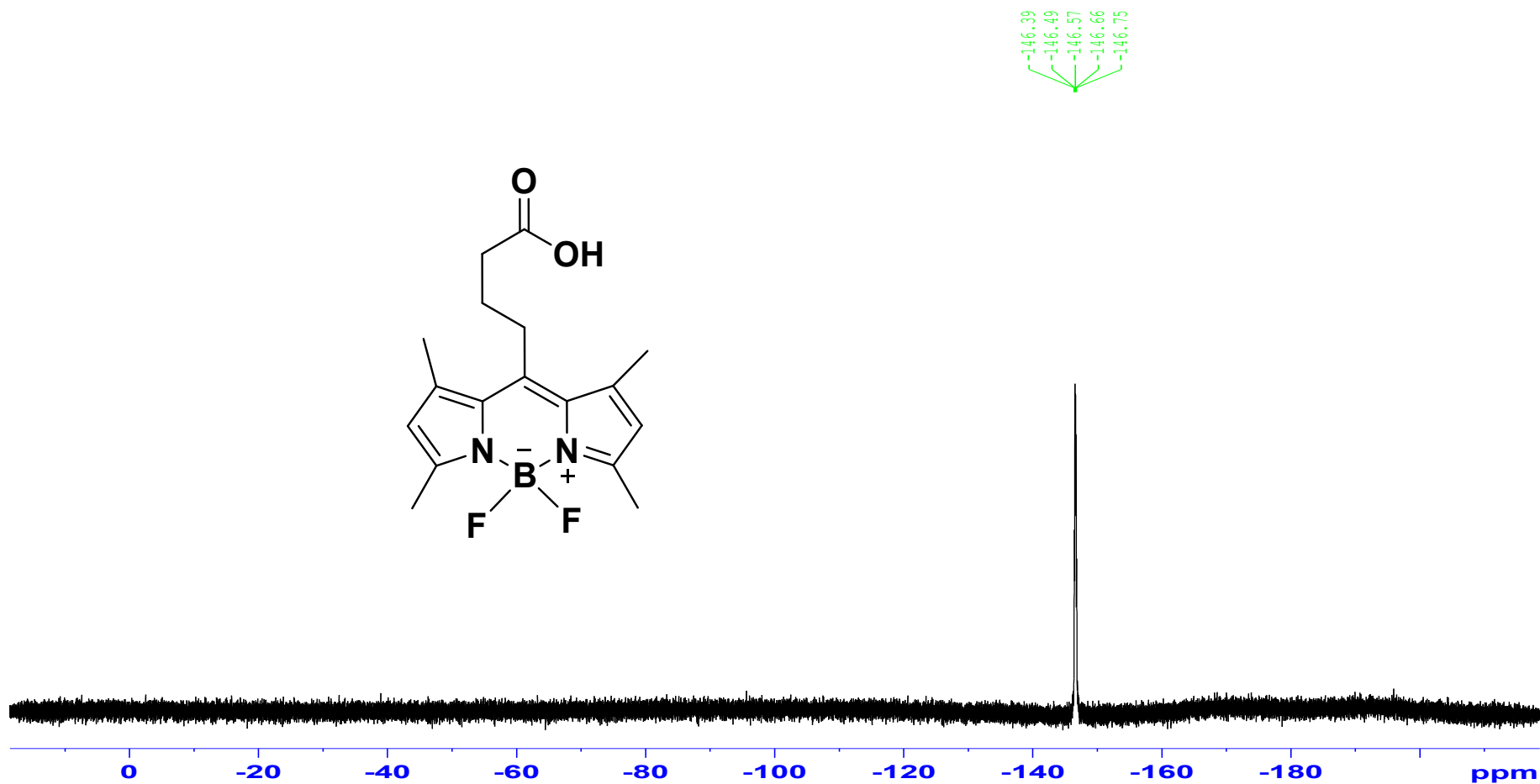


Figure 17: ^{19}F NMR spectrum of 4-(4,4-Difluoro-1,3,5,7-tetramethyl-4-bora-3a,4a-diaza-s-indacene-8-yl)-butyric Acid (4)

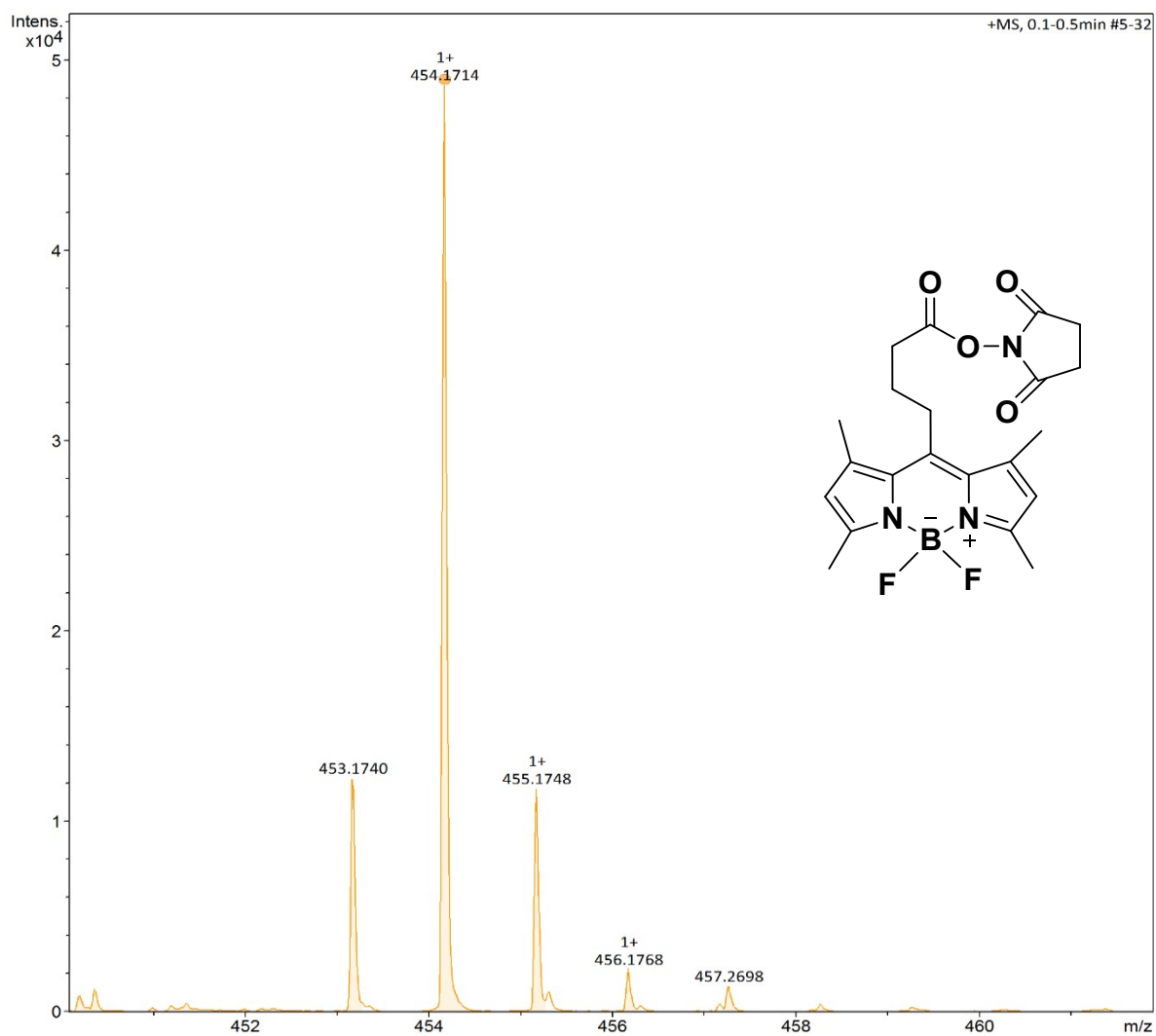


Figure 18: HRMS spectrum for 4-(4,4-Difluoro-1,3,5,7-tetramethyl-4-bora-3a,4a-diaza-s-indacene-8-yl)-butyric succinimidyl Ester (**8**)

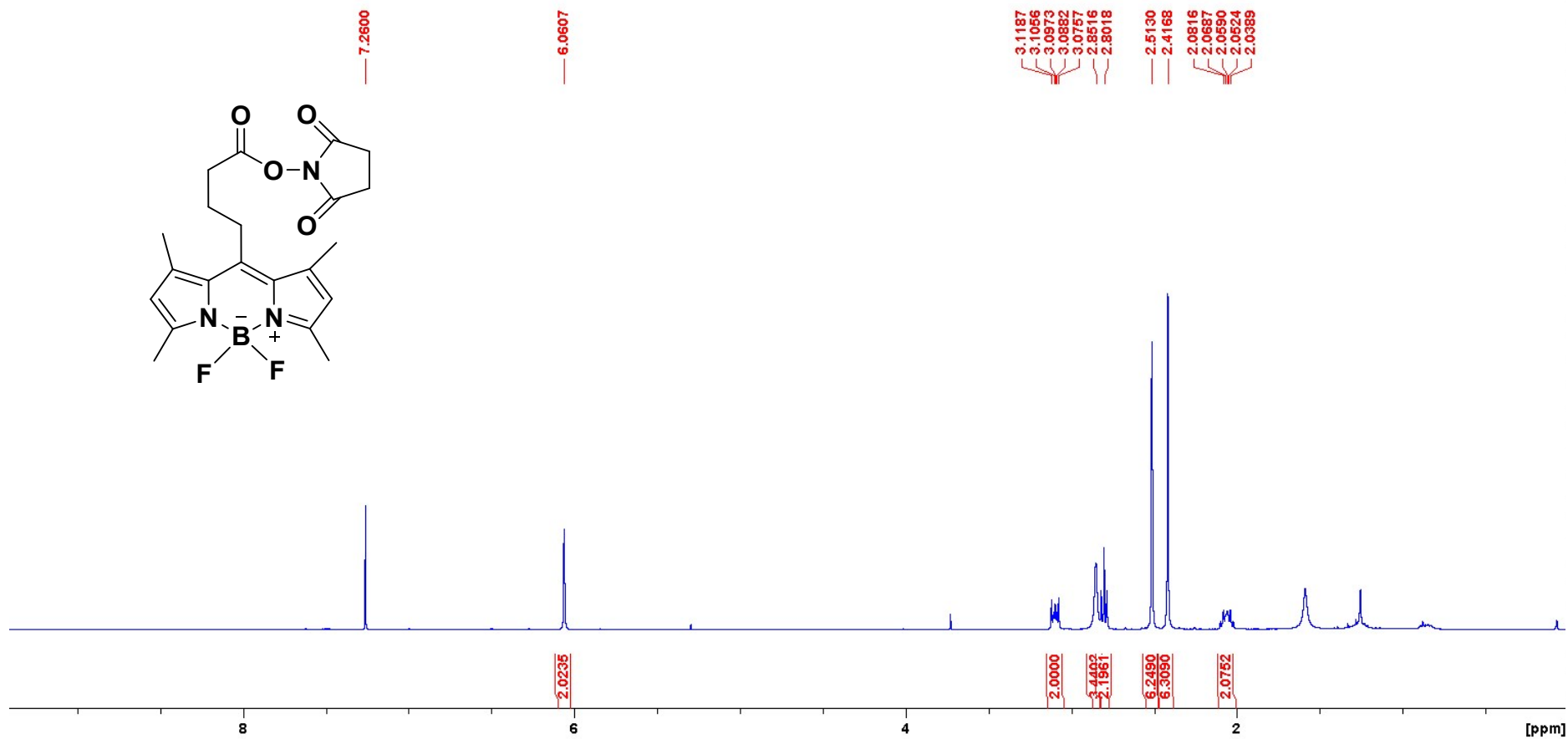


Figure 19: ¹H NMR spectrum of 4-(4,4-Difluoro-1,3,5,7-tetramethyl-4-bora-3a,4a-diaza-s-indacene-8-yl)-butyric succinimidyl Ester (**8**)

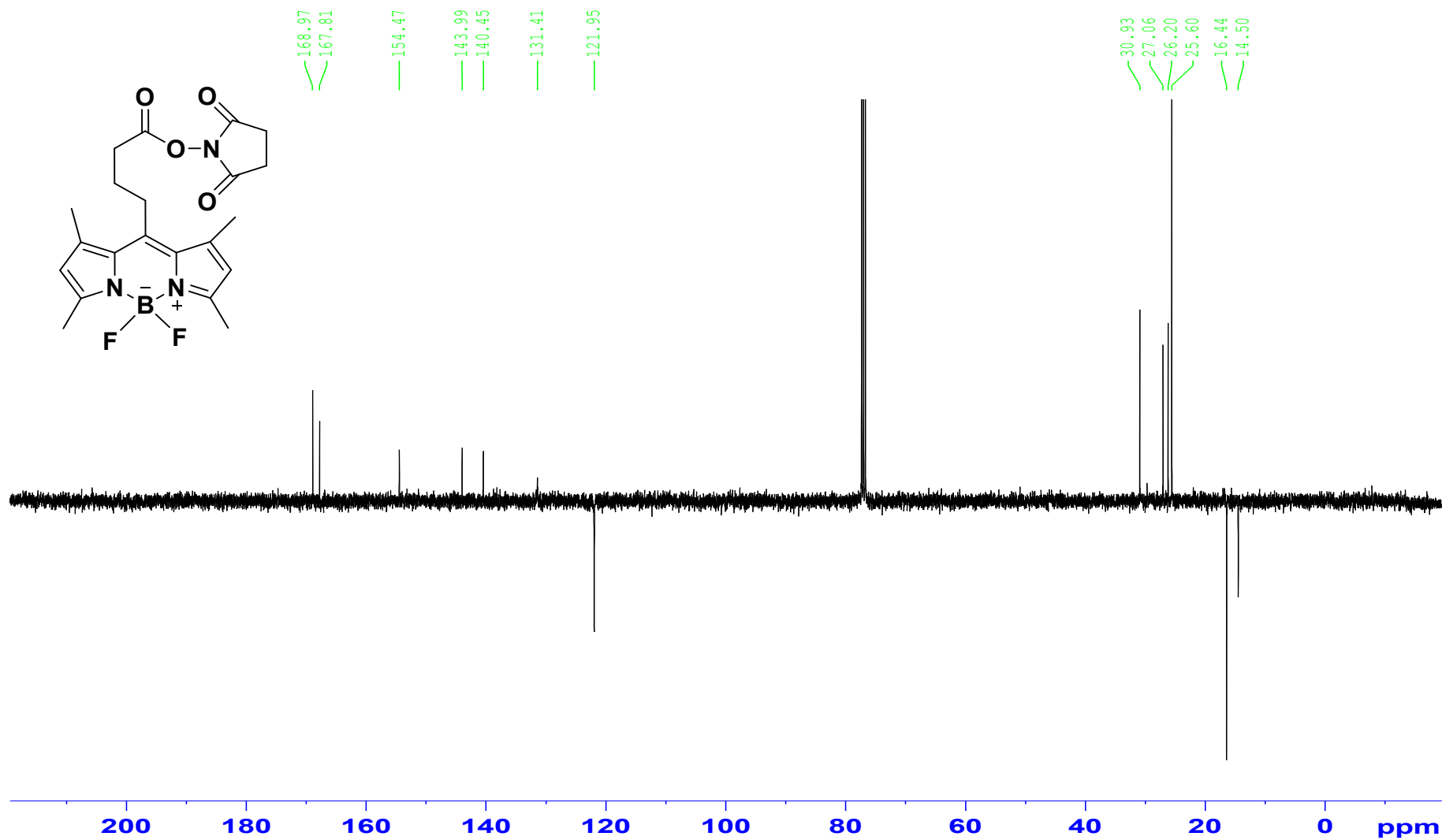


Figure 20: ¹³C NMR spectrum of 4-(4,4-Difluoro-1,3,5,7-tetramethyl-4-bora-3a,4a-diaza-s-indacene-8-yl)-butyric succinimidyl Ester (**8**)

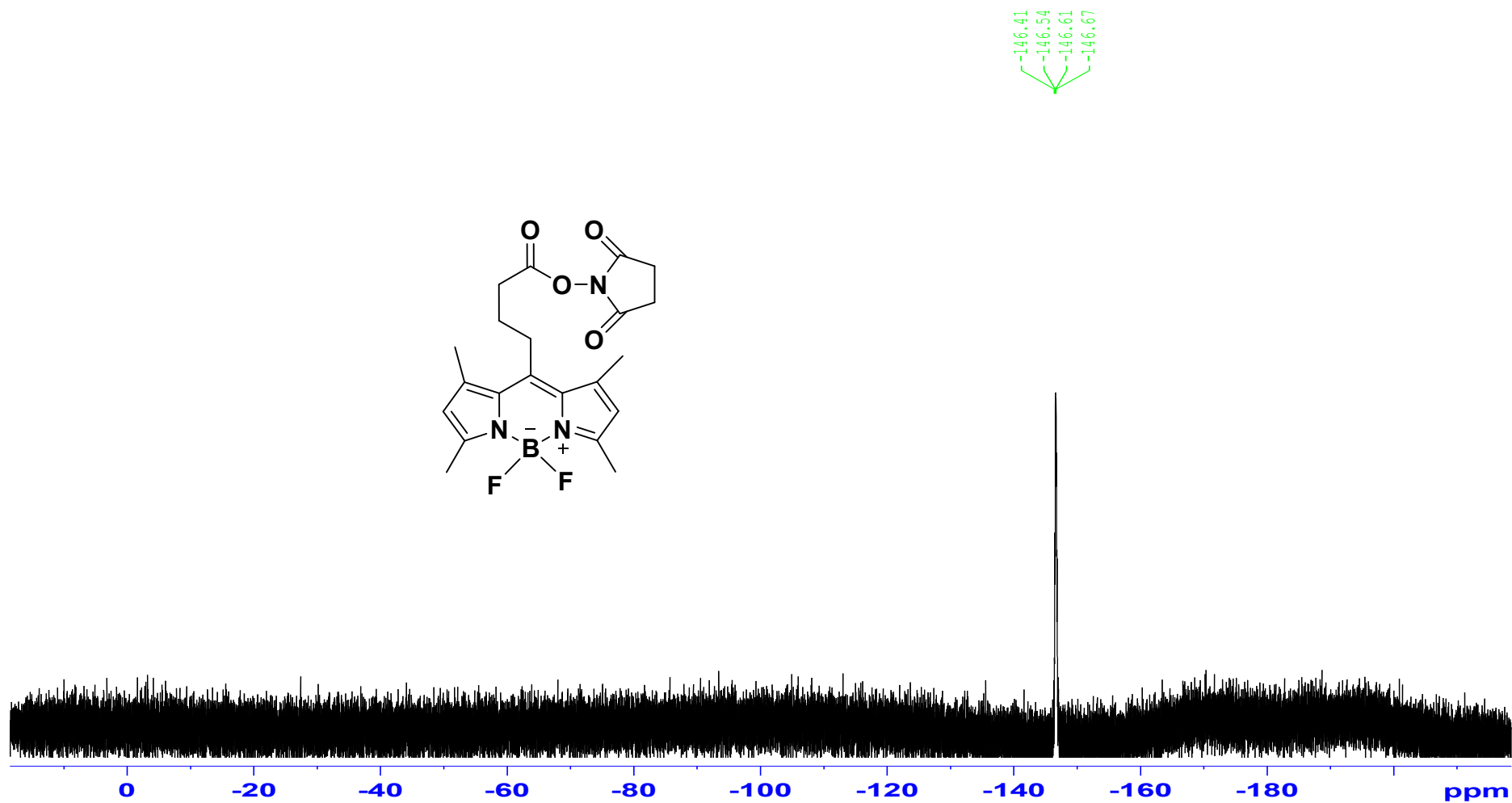


Figure 21: ^{19}F NMR spectrum of 4-(4,4-Difluoro-1,3,5,7-tetramethyl-4-bora-3a,4a-diaza-s-indacene-8-yl)-butyric succinimidyl Ester (**8**)

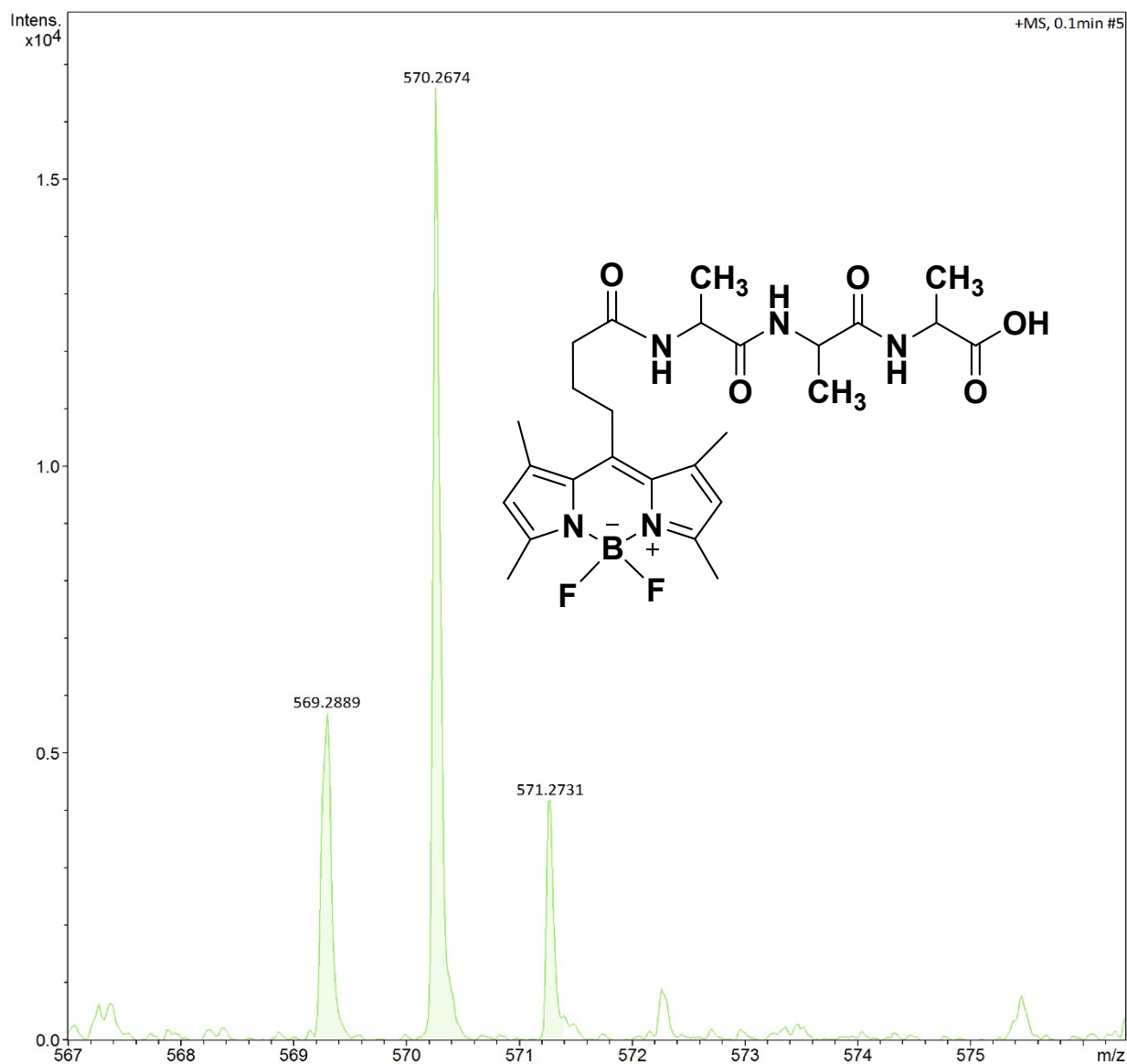


Figure 22: HRMS spectrum for 4-(4,4-Difluoro-1,3,5,7-tetramethyl-4-bora-3a,4a-diazas-indacene-8-yl)-butyricamide-Ala-tripeptide (**9**) with Na⁺ adduct.

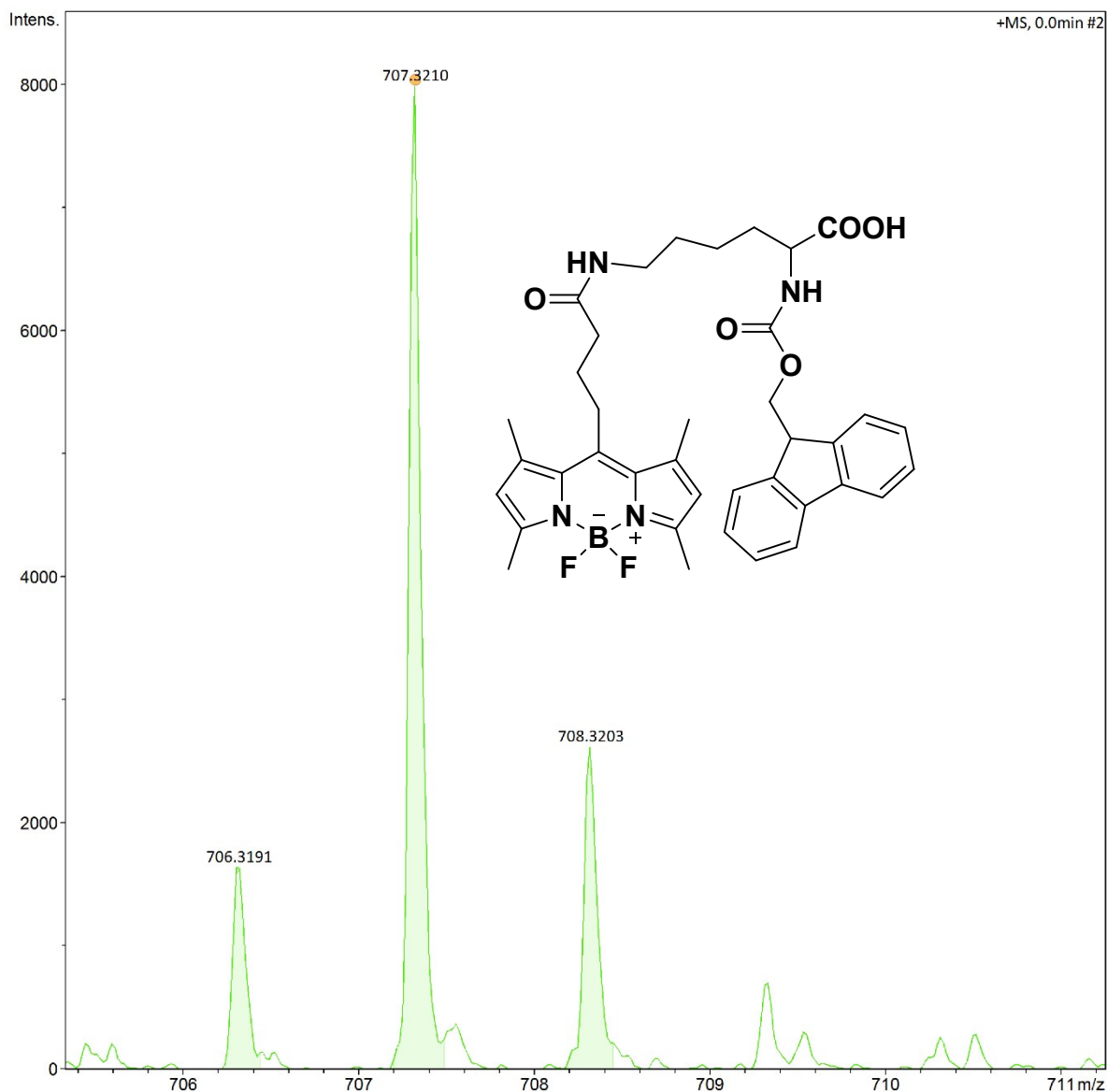


Figure 24: HRMS spectrum for Fmoc-Lys(4-(4,4-Difluoro-1,3,5,7-tetramethyl-4-bora-3a,4a-diaza-s-indacene-8-yl)butyricamide) peptide (**10**) with sodium adduct

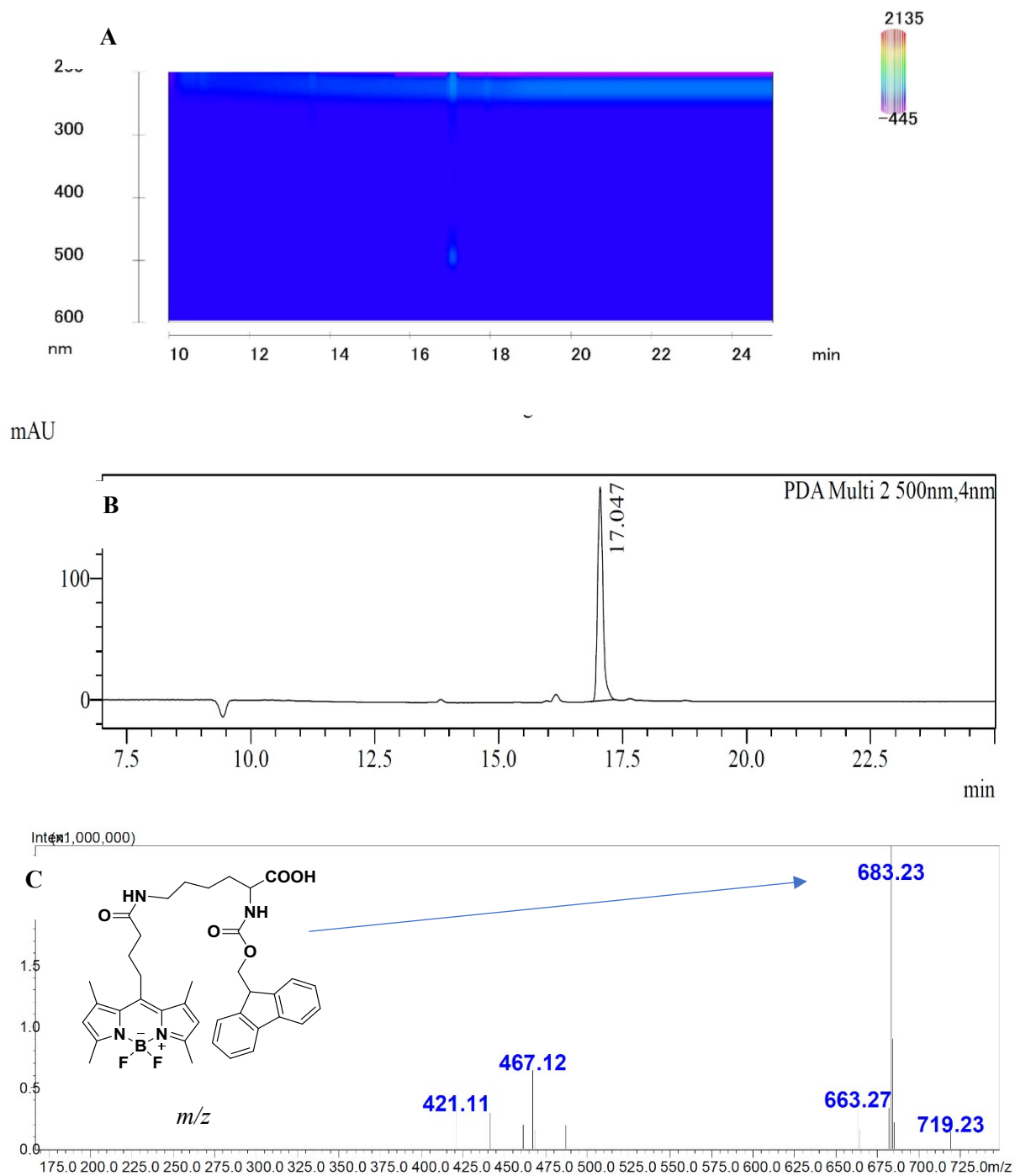


Figure 25: LC-MS-PDA chromatogram of **10**. **A** PDA showing the purity, **B** LC with retention time and **C** is the MS with the mass in $[M-H]^-$

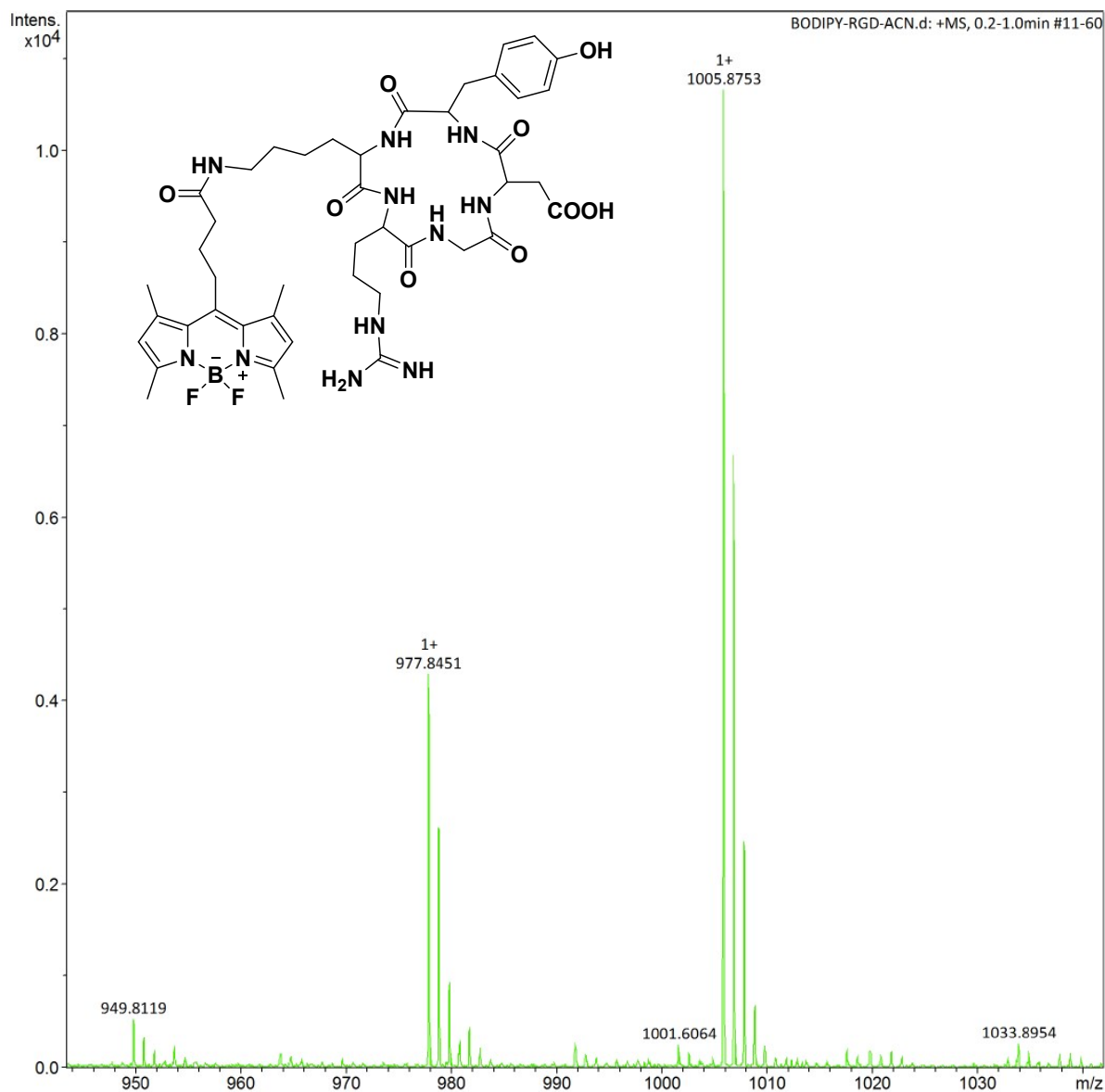


Figure 26: HRMS spectrum for 4-(4,4-Difluoro-1,3,5,7-tetramethyl-4-bora-3a,4a-diaza-s-indacene-8-yl)-butyricamide cyclic RGD peptide (**11**) with acetonitrile adduct

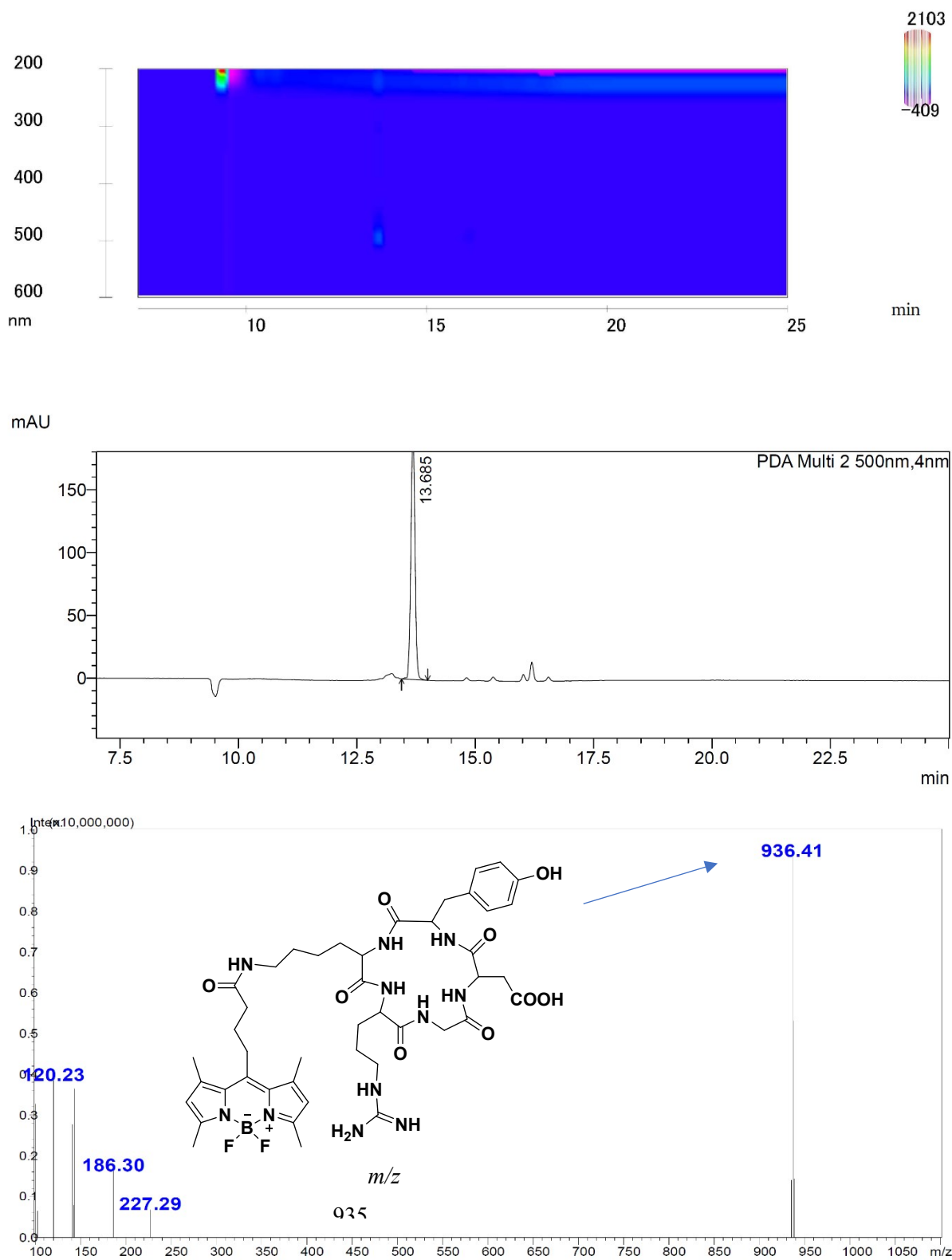


Figure 27: LC-MS-PDA chromatogram of **11**. **A** PDA showing the purity, **B** LC with retention time and **C** is the MS with the mass in $[M+H]^+$